

RESEARCH ARTICLE

Treatment of AL-Diwaniyah Petroleum Refinery Wastewater by Heterogeneous Fenton – Like Using Fe₂O₃ @ CeO₂; 1:2 Ratio /AC Nanocatalyst

Saleem F. Mones¹, Husham M. Al-Tameemi², Rafid K. Abbas^{3*}, Zahraa M. Ghafil⁴

University of Al-Qadissiyah-College of Engineering -Chemical Engineering

*Corresponding author: Rafid K. Abbas; Rafid.Abbas@qu.edu.iq

ABSTRACT

In present work, a heterogeneous Fenton process using prepared Fe₂O₃@ CeO₂; 1:2 ratio /AC nanocatalyst was used to treat wastewater discharged from Iraqi petroleum refinery plant. The heterogeneous Fenton process was evaluated for its efficiency in removing COD via application a response surface methodology (RSM) and adopting a batch mode. Three essential operating factors were considered namely catalyst dosage (0.5-1.5 g/l), H₂O₂ dosage (0.4-1), and pH (3-7). The Fe₂O₃@ CeO₂; 1:2 ratio /AC nanocatalyst was characterized using XRD, FESEM. EDS techniques. Results showed good adhesion property of the prepared nanomaterials with nano size with particle size diameter in range of (31.52- 69.08 nm). The optimum operating conditions were: catalyst dosage of 1.5 g/l, H₂O₂ dosage of 0.5878 g/l and pH of 3 in which RE% of 85% was achieved. Results of ANOVA confirmed that the catalyst dosage has the most significant effect on RE% with a contribution of 57.66% followed by pH is 22.03%, and H₂O₂ dosage is 11.91%. The comparison between the classical Fenton processes with heterogeneous Fenton process (Fenton- Like) showed that higher removal efficiency could be achieved using the heterogeneous Fenton process conferring the importance of application this processes as an alternative, sustainable, and cost-effective processes in the treatment of petroleum wastewaters.

Keywords: Petroleum refinery wastewater; heterogeneous Fenton process; Fe₂O₃; Fenton- Like; CeO₂.

ARTICLE INFO

Received: 13 March 2026
Accepted: 13 May 2026
Available online: 18 June 2026

COPYRIGHT

Copyright © 2025 by author(s).
Applied Chemical Engineering is published by
Arts and Science Press Pte. Ltd. This work is
licensed under the Creative Commons
Attribution-NonCommercial 4.0 International
License (CC BY 4.0).
<https://creativecommons.org/licenses/by/4.0/>

1. Introduction

Water is vital for life on the planet, acting as a basic need for all living beings. The rapid growth in population can be attributed to quick automation and economic development. The petroleum industries and refineries play a crucial role in the contribution of economic growth [1].

The problem of waste/wastewater disposal is an important challenge encountered by petroleum refineries and petrochemical plants. The wastewater discharged by petroleum industries is known to contain a combination of organic, inorganic pollutants, heavy metals, phenol, hydrocarbons, and sulfides. The petroleum industry emits considerable quantities of hazardous pollutants from different sectors, involving oil production, transportation, refining, petrochemical manufacturing, storage, and distribution which have negative effects on the environment as well as human health [2-4].

The treatment of petroleum refinery wastewater (PRW) includes many traditional techniques, such as physical, chemical, and biological processes. However, these traditional processes are considered non-efficient and cannot completely degrade all pollutants [5].

Recently, Electrochemical processes and advanced oxidation processes (AOPs) have been considered an alternative to conventional treatment processes. Fenton-based processes is an example of AOPs that have shown great efficacy in breaking down many pollutants that are otherwise hard to eliminate through traditional processes [6-8]. The Fenton reaction produces hydroxyl free radicals $\text{OH}\cdot$, which results from the interaction between ferrous ions (Fe^{2+}) and hydrogen peroxide (H_2O_2). According to Hassan et al. (2018), $\text{OH}\cdot$ is a powerful oxidizing agent that efficiently decomposes all organic pollutants, forming CO_2 , H_2O , and inorganic salts [7-9].

Although the potential of the classical Fenton process for wastewater treatment, it has several limitations that limit its practical application. The disadvantages include the substantial volumes of sludge iron, elevated costs of operation, and challenges associated with the regeneration of catalysts [6].

Heterogeneous Fenton procedures have been effectively used to treat wastewater from the petrochemical, textile, pharmaceutical, and refinery industries, where traditional techniques frequently fall short of removing enough pollutants. The immobilized catalysts improve process scalability and efficiency by facilitating incorporation into fixed-bed or fluidized-bed reactors in addition to enhancing stability. Heterogeneous Fenton wastewater treatment, which combines the tremendous oxidative effect of hydroxyl radicals with useful enhancements in catalyst handling and process sustainability, is a noteworthy development in environmental engineering. It is therefore a viable way to deal with the problems caused by refractory industrial effluents [10-11].

With an emphasis on catalyst design, reaction efficiency, and pollutant degradation pathways, the current study explores the use of heterogeneous Fenton-based treatment for effluent from petroleum refineries. By immobilizing iron on solid supports, heterogeneous catalysts reduce secondary pollution and sludge formation. In contrast to homogeneous systems that use iron salts, solid catalysts in heterogeneous systems can be recovered and reused several times, increasing sustainability and cost-effectiveness [12-13].

The study illustrates the possibilities for industrial-scale application of heterogeneous catalysts by investigating their performance under actual operating conditions. In line with international initiatives to lessen environmental impacts and encourage cleaner production in the petroleum sector, the study adds to the expanding corpus of information on sustainable wastewater treatment.

The aim of this work is to examine the feasibility of heterogeneous Fenton process using $\text{Fe}_2\text{O}_3 @ \text{CeO}_2$; 1:2 ratio /AC as nanocatalyst in system operated at batch mode with a suspension configuration of catalytic reactor. Impact of operating variables such as catalyst dosage (C.D), dosage of H_2O_2 dosage and, pH, on removal of COD from wastewater generating from Al-Diwaniyah petroleum refinery plant was investigated by adopting response surface methodology (RSM). Adopting batch- mode in the present work is based on its successful application in treatment of various wastewaters. Using experimental design in this work was preferred since the conventional procedure (one-factor-at-a-time) has no ability to find effects of interaction among the variables which could be effective on the efficiency of process. Besides, reducing a number of runs, lowering the cost and short time of performing the experiments can be obtained via RSM.

2. Materials and techniques

2.1. Features of wastewater from petroleum refineries

Al-Diwaniyah refinery in south of Iraq was functioned as the case study for the present research. For the purpose of the pilot program, 40 liters of the wastewater were removed from the feed tank prior to the biological treating unit and stored at 4°C . A filtration stage was carried out using a Puchner filter with Whatman filter paper (grade 1) with a pore size of $11\ \mu\text{m}$ in order to decrease the suspended particles present in the effluent.

The characteristics of the biological unit's treated effluent and the untreated wastewater supplied by the plant administration are shown in **Table 1**.

Table 1. Characterization of wastewater discharged from Al-Diwaniyah refinery plant

Characteristic	pH	Temperature °C	BOD Ppm	COD ppm	TDS ppm	Phenol ppm	Oil content	Turbidity NTU	PO ₄ ³⁻ ppm	Cl ⁻ ppm
Value	7.1	12	180	776	5560	18.5	74.8	117	0.12	900

2.2. Chemicals

Various chemicals were used in the present work obtained from different resources. Fe₂O₃ nanoparticles with sizes between 10 and 30 nm were used as a nanocatalyst. It was purchased from (SkySpring Nanomaterials Inc., Houston, USA). CeO₂ nanoparticles with a size range of 10 – 30 nm were used as an imported nanocatalyst from the United Kingdom. Activated carbon used in the tests as adsorption media were produced from FINE CHEM LIMITED, India. The source of hydrogen peroxide (H₂O₂) is from UK and used as a source of OH⁻. Ethanol, and phenol were used for experimental runs. These materials originated from MilliporeSigma US. To control the pH level and base action, sodium hydroxide was used (NaOH) (97.5 % Thomas Baker, India). To change the pH to an acidic effect, hydrochloric acid (37 – 38 %, TEDIA COMPANY, INC, US) was utilized. Distilled water was purchased from local source.

2.3. Preparation of Fe₂O₃- CeO₂; 1:2 ratio /AC nanocatalyst

In this study, Fe₂O₃- CeO₂; 1:2 ratio /AC nanocatalyst was prepared according to the method in work of Ahmadreza Yazdanbakhsh, et al.,2018 [14]. The first stage includes activation process for activated carbon. The activated carbon was initially screened using a 0.5 – 0.8 mm sieve. A 5% hydrochloric acid (HCl) solution was prepared utilizing the normality law. Subsequently, 100 g of the screened activated carbon was soaked in the HCl solution for a period of 24 hours. Following this treatment, the sample was washed with distilled water until the pH value reached 6. Finally, the activated carbon was dried in an oven at 100° C for 6 hours. The second stage include take 1 g of activated carbon (AC) was placed into a 250 ml beaker, followed by the addition of 250 ml of distilled water. Subsequently, 0.2 g of Fe₂O₃ and 0.26 g of CeO₂ nanomaterials were introduced into the mixture. The suspension was then agitated using a magnetic stirrer for 30 minutes to ensure thorough mixing. After the stirring process, the contents were washed three times with ethanol and filtered using a Buchner funnel equipped with a vacuum pump. The resulting solid was dried in an oven at 100° C for 6 hours. Finally, the prepared sample was stored in a closed vessel for preservation. Figure 1. illustrates the preparation procedure [14-15].

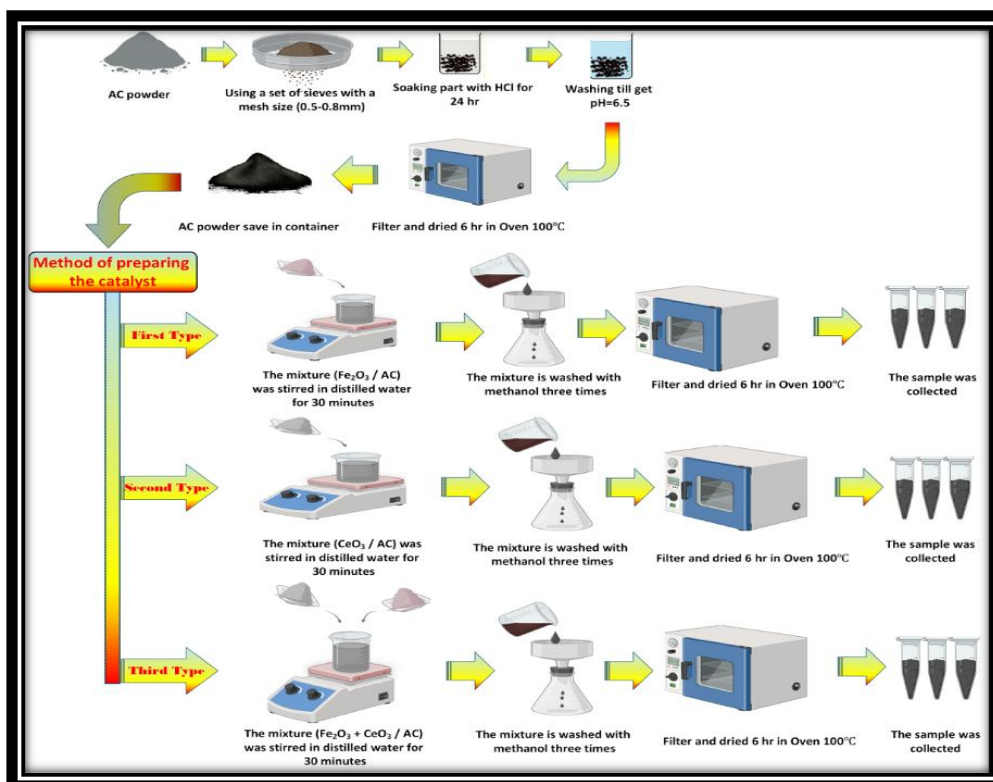


Figure 1. General steps of $\text{Fe}_2\text{O}_3@\text{CeO}_2/\text{AC}$ preparation

2.4. The heterogeneous Fenton system

The heterogeneous Fenton system is depicted in **Figure 2**, where a batch Fenton oxidation mode process includes a glass beaker having dimensions (130 mm × 90 mm) with a capacity of 0.5 liter located on magnetic hotplate stirrer to treat the petroleum refinery wastewater with $\text{Fe}_2\text{O}_3@\text{CeO}_2$ nanoparticles loaded on activated carbon at ratio 1:2.

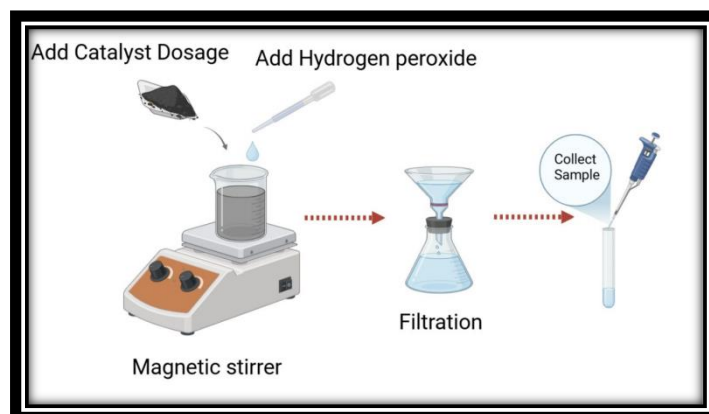


Figure 2. Heterogeneous Fenton system

2.5. Characterizations and analytical Methods

X-ray thin film diffractometer (XRD 6000 /Shimadzu/ Japan) with $\text{CuK}\alpha$ radiation of 1.5405 Å was functioned to identify the phase structure of $\text{Fe}_2\text{O}_3@\text{CeO}_2/\text{AC}$ with testing 2θ at range $20\text{--}80^\circ$. With a step size of 0.2 degrees, the scan step time was 1.2 seconds. The XRD was run at 30 mA and 40 kV. The morphology and microstructure of TiO_2 nanoparticles and SnO_2 anode were analyzed using SEM (Model: TESCAN-VEGA/USA).

COD is a precise technique used in wastewater treatment to identify the organic and inorganic chemicals that make up wastewater. This test can determine the concentration of these chemicals based on the total amount of oxygen required to oxidize them and turn them into CO₂ and H₂O. In order to validate the hybrid process and its ability to incinerate organic contaminants in effluent from petroleum refineries, COD removal was used in the current work. The test involves placing 2 milliliters of wastewater in a thermal reactor (RD125, Lovibond, Germany) for 120 minutes at 150 degrees Celsius, then digesting it with an oxidizing agent (K₂Cr₂O₇). The COD value was determined using a spectrophotometer (MD200, Lovibond, Germany) after the sample had cooled to room temperature. The solution conductivity was measured using a conductivity tester (HANNA Instrument Inc., Romania), and a digital pH meter (HANNA Instrument Inc. Romania) was utilized to gauge the solution's pH.

2.6. Performance evaluation

Chemical oxygen demand (COD) efficiency was determined using Eq. 1 to determine the combined process's performance ^[16]:

$$RE\% = \frac{COD_i - COD_f}{COD_i} \times 100 \quad (1)$$

In this equation, RE% indicates COD removal effectiveness, COD_i and COD_f stand for the initial and final COD values, respectively (mg/L).

2.7. Experimental design

Response surface methodology (RSM) is a set of statistical and mathematical techniques for optimizing the response's operational circumstances, which are impacted by different process operating variables. One of the best designs utilized in RSM to validate and test the process parameters that affected the removal of COD was the Box-Behnken design (BBD), which has three components and three levels.

In the BBD, four process variables were considered as process factors namely catalyst dosage C.D (X₁), H₂O₂ dosage (X₂), and pH (X₃) with their coded levels as -1 (low level), 0 (middle point), and +1 (high level) while RE% was considered as a response ^[17]. **Table 2** displays the process variables with their chosen levels.

Table 2. Variables in the refinery wastewater treatment process and their values

Procedure parameters	Box-Behnkon Design Range		
	Low (-1)	Middle (0)	High (+1)
Levels of coding			
X ₁ : H ₂ O ₂ (g/l)	0.4	0.7	1
X ₂ : Catalyst Dosage (g/l)	0.5	1	1.5
X ₃ : pH	3	5	7

Using a fraction of the chosen runs for a three-level factorial, Box-Behnken provides the necessary designs to create the proper quadratic model with the acceptable statistical requirements. The following equation can be used to estimate the number of runs (N) required to complete a Box - Behnken design ^[17-19]:

$$N = 2k(k - 1) + cp \quad (2)$$

Where variables number is represented by (k) and number of repeating the central point by (cp).

Based on Eq. (4), 27 runs should be performed to identify the interactions among variables and their impacts on the removal efficiency. Table 3 displays the BBD array proposed for this study.

A second order polynomial model could be formulated based on BBD as shown in Eq.3 ^[17-19]:

$$Y = a_0 + \sum a_i x_i + \sum a_{ii} x_i^2 + \sum a_{ij} x_i x_j \quad (3)$$

according to Eq.5, the COD removal could be represented as a response (Y) and $x_1, x_2 \dots x_k$ represent the process factors. a_0 is intercept term, (i) and (j) denotes the index numbers for patterns. The first order main effect is represented by a_i , the second order main effect by a_{ii} , and the influence of interactions by a_{ij} . To assess the model's fit, a regression coefficient (R^2) is calculated.

3. Results and Discussion

3.1. Characterizations of (Fe₂O₃@CeO₂; 1:2 ratio)/AC

3.1.1. (Fe₂O₃@CeO₂; 1:2 ratio)/AC XRD Test

Iron oxide and Cerium dioxide supported on activated carbon (Fe₂O₃@CeO₂; 1:2 ratio)/AC is an important type catalyst material that has drawn a lot of attention due to its excellent structural, optical, electrical, and thermal properties. **Figure 3** shows The XRD pattern of the (Fe₂O₃@CeO₂;1:2 ratio)/AC Nano catalyst confirms the presence of cubic CeO₂ and rhombohedral Fe₂O₃ phases. The characteristic diffraction peaks of CeO₂ at $2\theta \approx 28.5^\circ, 33.1^\circ, \text{ and } 47.5^\circ$ are dominant due to its higher loading ratio, while Fe₂O₃ peaks appear with lower intensity. A broad diffraction band around $23 - 26^\circ$ corresponds to amorphous activated carbon. The absence of impurity peaks indicates successful immobilization of metal oxides on the AC support. Similar observation was observed by [Huizhi Bao et al.](#) [20-23].

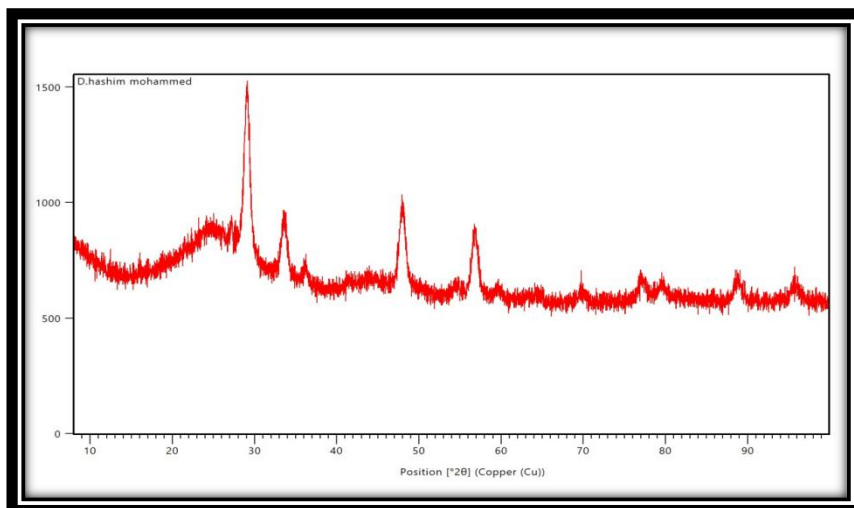
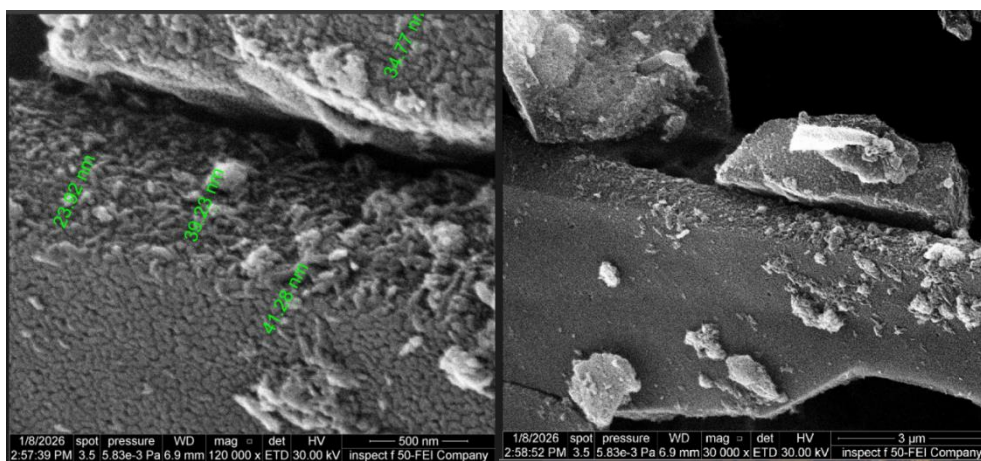


Figure 3. XRD pattern for nanoparticle of (Fe₂O₃@CeO₂; 1:2 ratio)/AC

3.1.2 (Fe₂O₃@CeO₂; 1:2 ratio) /AC FESEM & EDS Test

Figure 4 shows FESEM images of (Fe₂O₃@CeO₂; 1:2 ratio)/AC nanoparticle at two magnification 120kX and 30kX. Images showed that (Fe₂O₃@CeO₂; 1:2 ratio)/AC nanoparticles reveal a highly porous and rough surface structure characteristic of activated carbon, providing abundant anchoring sites for metal oxide nanoparticles. The range of particle sizes in figure (4-a) was found to be between 23.2 and 41.28 nm, proving their nanoscale. The BET Surface Area of CeO₂/AC was determined to be 600 m²/g and the BET Surface Area of (Fe₂O₃@CeO₂; 1:2 ratio) /AC was 571 m²/g. The average pore diameter and volume for (Fe₂O₃@CeO₂; 1:2 ratio) /AC was determined to be 6 nm and 0.61 cm³/g (p/p₀=0.990), respectively. The reduction in surface area after loading the metals is a typical phenomenon observed by [Naife et al.](#) [24] due to pore-filling.



(a) (b)

Figure 4. SEM images of (Fe₂O₃- CeO₂; 1:2 ratio)/AC nanoparticles. a) magnification 12kX, b) magnification

Table 3 and **Figure 5** summarize the energy-dispersive X-ray spectroscopy (EDS) for Fe₂O₃@CeO₂; 1:2 ratio)/AC. After analysing the obtained results, it can be seen that Fe, Ce, O, and C elements in the prepared catalyst have the oxidation ability for organic pollutants in wastewater.

Table 3. DES elemental analysis of (Fe₂O₃- CeO₂; 1:2 ratio)/AC

Element	Atomic %	Atomic % Error	Weight %	Weight % Error
C	82.2	1.2	70.9	1.0
O	16.0	1.1	18.4	1.3
Fe	1.1	0.1	4.3	0.6
Ce	0.6	0.1	6.4	0.8

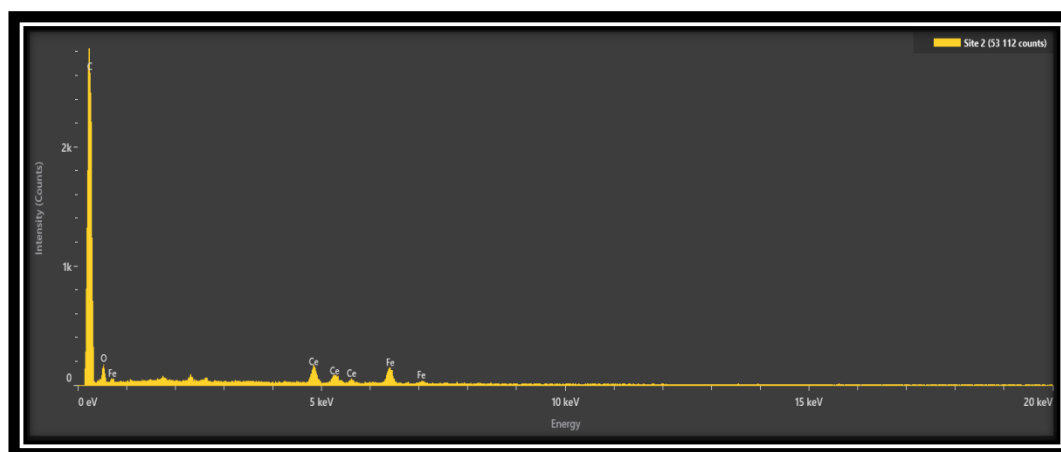


Figure 5. EDS of (Fe₂O₃- CeO₂; 1:2 ratio)/AC

3.1.3 (Fe₂O₃@CeO₂; 1:2)/AC FTIR Test

Figure 6 demonstrates the FTIR results of (Fe₂O₃@CeO₂; 1:2 ratio)/AC nanoparticles. Functional groups present in the structure of the nano catalysts were determined by Fourier transform infrared spectroscopy. The Fourier-transform infrared spectroscopy (FT-IR) analyses of the nano catalysts were run with Bomem MB-Series FT-IR Spectrometer. The characteristic stretching band for activated carbon bands is O - H stretching: Broad band around 3400 - 3600 cm⁻¹, due to hydroxyl groups or adsorbed water, C=C stretching (aromatic rings): Around 1500 - 1600 cm⁻¹, and C - O stretching: 1000 - 1300 cm⁻¹, associated with alcohols, ethers,

or phenols. While for Fe_2O_3 Bands the results identified the Fe - O stretching vibrations are usually in the $400 - 600 \text{ cm}^{-1}$ region, at $\sim 540 - 580 \text{ cm}^{-1}$ corresponds to Fe - O vibrations of hematite (Fe_2O_3), and a weaker band around $470 - 500 \text{ cm}^{-1}$ may appear for maghemite or other iron oxide phases. For CeO_2 band is $400 - 600 \text{ cm}^{-1}$ is Ce - O stretching vibrations (fluorite structure). The FTIR results agreed with the results obtained by Mariana Riboli Navaa [25].

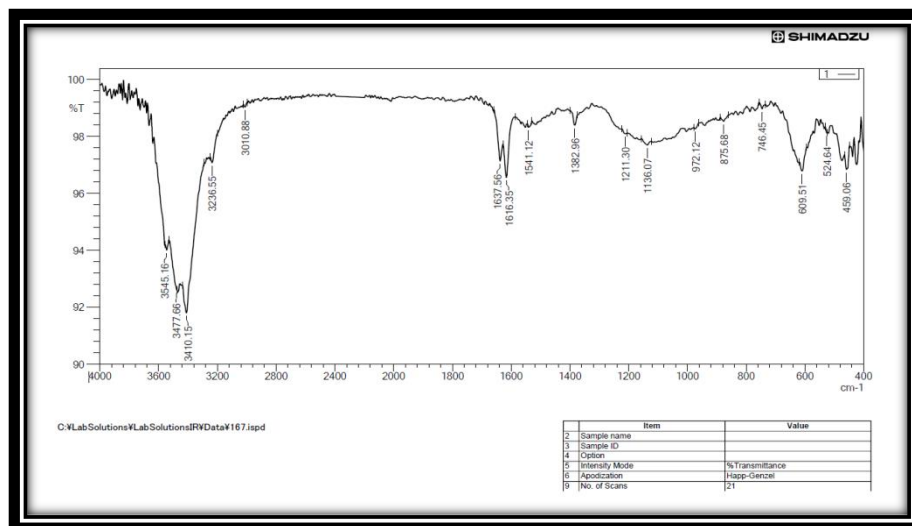


Figure 6. FTIR image of $(\text{Fe}_2\text{O}_3@ \text{CeO}_2; 1:2 \text{ ratio})/\text{AC}$

3.2. Catalyst Activation by Simulated Wastewater

Activation of the prepared catalyst was carried out for five types of catalysts and these catalysts $\text{Fe}_2\text{O}_3/\text{AC}$, CeO_2/AC , $\text{Fe}_2\text{O}_3@ \text{CeO}_2; 2:1 \text{ ratio}/\text{AC}$, $\text{Fe}_2\text{O}_3@ \text{CeO}_2; 1:1 \text{ ratio}/\text{AC}$, and $\text{Fe}_2\text{O}_3@ \text{CeO}_2; 1:2 \text{ ratio}/\text{AC}$ to evaluate their effectiveness in treating organic pollutants. A two-hour experiment was conducted to treat simulated wastewater (distilled water contaminated with phenol concentration 100 ppm has initial COD = 442 ppm) in which 250 ml of simulated wastewater was placed in a beaker under the conditions described below and stirred using a magnetic stirrer under the conditions (catalyst dosage 0.25 g/ 250 ml, Temperature = 25°C , and pH = 3. Samples of the treated liquid were taken every 30 minutes, and the chemical oxygen demand (COD) was determined. The catalyst that achieved the highest COD removal efficiency was selected, as shown in Table 4 below.

Table 4. Activation processes using five types of prepared nanocatalyst

No.	Catalyst Type	$\text{COD}_r(\text{ppm})$			
		30 min	60 min	90 min	120 min
1	AC alone	440	412	405	401
2	$\text{Fe}_2\text{O}_3/\text{AC}$	391	369	330	314
3	CeO_2/AC	338	376	371	398
4	$\text{Fe}_2\text{O}_3@ \text{CeO}_2; 2:1 \text{ ratio}/\text{AC}$	330	301	288	255
5	$\text{Fe}_2\text{O}_3@ \text{CeO}_2; 1:1 \text{ ratio}/\text{AC}$	305	295	259	243
6	$\text{Fe}_2\text{O}_3@ \text{CeO}_2; 1:2 \text{ ratio}/\text{AC}$	262	248	226	208

From these runs, the results illustrated that the catalyst ($\text{Fe}_2\text{O}_3- \text{CeO}_2; 1:2 \text{ ratio}/\text{AC}$) has the highest removal is 208 ppm at 120 min therefore; this catalyst was selected for use in the wastewater treatment in petroleum refineries, which will be discussed in the following section.

The limited efficiency of CeO₂/AC alone (COD = 398 ppm) can be explained by the weak catalytic role of CeO₂ as an independent Fenton catalyst under the given conditions. Although CeO₂ contains a reversible Ce³⁺/Ce⁴⁺ redox system, it is not highly effective in directly activating H₂O₂ to generate hydroxyl radicals (•OH), especially when compared with iron-based catalysts. In addition, CeO₂ may favor side reactions that lead to the non-productive decomposition of H₂O₂, or primarily function as an oxygen storage material rather than an active catalytic center, which results in minimal or even negative impact on COD removal.

On the other hand, Fe₂O₃/AC exhibits moderate catalytic performance (COD = 314 ppm) because of its capability to produce •OH radicals through the Fe²⁺/Fe³⁺ Fenton cycle. However, its activity is constrained by the relatively slow reduction of Fe³⁺ back to Fe²⁺, limiting the (continuous) generation of reactive radicals.

A marked improvement is observed with the CeO₂ - Fe₂O₃/AC (1:2) composite catalyst (COD = 208 ppm), which is attributed to a synergistic interaction between the two oxides rather than a simple physical combination. This enhancement can be explained by several factors. First, the redox interaction between Ce³⁺/Ce⁴⁺ and Fe³⁺/Fe²⁺ accelerates the regeneration of Fe²⁺, thereby promoting sustained •OH production. Second, the presence of oxygen vacancies in CeO₂ enhances electron transfer at the interface with Fe₂O₃. Third, coupling CeO₂ with iron sites improves the efficiency of H₂O₂ activation and reduces undesired decomposition pathways. Finally, the mixed oxide system likely achieves better dispersion on activated carbon, increasing the availability and accessibility of active sites.

Overall, the superior catalytic performance of the combined system arises from a true synergistic mechanism, where CeO₂ functions as a redox mediator that enhances the intrinsic Fenton activity of Fe₂O₃, rather than acting as an independent catalyst.^[26]

3.3. Removal of COD by (Fe₂O₃@CeO₂; 1:2 ratio)/AC nanocatalyst

3.3.1. RSM results

According to the parameters being effected (catalyst dosage, H₂O₂ dosage, pH, and time), the design of experiments would be more complicated and take long time, therefore, the parameters will be shortened to only three (catalyst dosage, H₂O₂ dosage, and pH) in order to simplify the design of experiments. A two-hour run has been done on petroleum refinery wastewater using the affected variables and the samples are chosen for each 30 min and COD test are measured for the chosen samples. Time has been selected to be fixed at 90 min that gave higher COD removal and at this time the affected parameters will be studied accordingly. The results of this run are illustrated in **Table 5** below.

Table 5. BBD design for PRWW using (Fe₂O₃@CeO₂; 1:2 ratio)/AC at middle conditions and fixed time

Middle Conditions			Time (min)	30	60	90	120
Fe ₂ O ₃ - CeO ₂ ; 1:2 ratio /AC dosage = 1 g/l	H ₂ O ₂ dosage = 0.7 g/l	pH= 5					
COD _r (ppm)				562	408	384	494

To examine the shared effects of the process factors on COD removal, fifteen experiments were conducted at different sets. **Table 6** displays the experimental data for RE% as well as the values anticipated by the model equation.

Table 6. Results of COD elimination utilizing a heterogeneous Fenton process with a nano catalyst of (Fe₂O₃@CeO₂; 1:2 ratio)/AC

StdOrder	Order of Runs	Pt Type	Blocks	H ₂ O ₂ (g/l)	Dosage of the Catalyst (g/l)	pH	COD _i =776 ppm		Pred.
							COD _r	RE%	
15	1	0	1	0.7	1.0	5	388	50	51.6667
10	2	2	1	1.0	1.0	3	364	53	55.2500
12	3	2	1	1.0	1.0	7	504	35	34.2500
14	4	0	1	0.7	1.0	5	388	50	51.6667
5	5	2	1	0.7	0.5	3	372	52	50.7500
2	6	2	1	0.4	1.5	5	233	70	71.0000
11	7	2	1	0.4	1.0	7	364	53	50.7500
9	8	2	1	0.4	1.0	3	287	63	63.7500
1	9	2	1	0.4	0.5	5	427	47	47.5000
6	10	2	1	0.7	1.5	3	116	85	83.2500
13	11	0	1	0.7	1.0	5	372	52	51.6667
7	12	2	1	0.7	0.5	7	489	37	38.7500
4	13	2	1	1.0	1.5	5	287	63	62.5000
3	14	2	1	1.0	0.5	5	528	32	31.0000
8	15	2	1	0.7	1.5	7	310	60	61.2500

Equation 1 below shows how a quadratic model based on the actual values of the process elements was created using Minitab-19 software:

$$\text{RE\%} = 61.2 - 4.7 X_1 + 30.5 X_2 - 5.46 X_3 + 17.67 X_1 X_1 - 34.3 X_2 * X_2 + 0.604 X_3 * X_3 + 13.33 X_1 * X_2 - 2.50 X_1 * X_3 - 3.33 X_2 * X_3 \quad (1)$$

Where X₁, X₂, X₃ act as process variables (Fe₂O₃@CeO₂; 1:2 ratio)/AC dosage, H₂O₂ dosage, and pH respectively while X₁X₂, X₁X₃ and X₂X₃ serve as these factors' interaction influence. A measure of the basic impact of the process variables is represented by (X₁)², (X₂)² and (X₃)². (+,-) signs in front of the system variables' coefficients and their interaction terms indicate antagonistic and synergistic effects.

The response model's (ANOVA) data is explained in **Table 7**, where DF stands for degree of freedom, Seq SS for sum of the square, Adj. SS for adjusted sum of the square, Adj. MS for adjusted mean of the square, and Contr. % for contribution for each factor. Fishers (F-test) and P-test were used to assess the model's capacity; a high Fisher value indicates that the regression equation may be utilized to fit the maximum boundaries of diversity. The (P-value) is used to assess whether F has a high value that is appropriate for differentiating the model's statistical significance. When the model's (P-value) is less than 5%, 95% of its variables can be discussed. The results of Table 4-6 indicate that the quadratic model, with an F-value of 52.12 at a confidence level over 95% (P-value equal to 0.000), is crucial. The lack of fit test can be used to determine whether the selected model adequately describes the data or whether a more comprehensive model is needed. When compared to the pure error, the (P-value) for lack of fit in the current work is equal to 0.1, which is greater than (0.05), indicating that it was not statistically significant. Consequently, the model is able to obtain a realistic prediction that matches the response values. The study's R² and adj. R² values were evaluated to be 0.989 and 0.97, respectively, indicating the congruence of the model-predicted and experimental results ^[26].

Table 7. ANOVA results of COD removal by heterogeneous Fenton process using (Fe₂O₃@CeO₂; 1:2 ratio)/AC nano catalyst

Source	DF	Seq. SS	Contr. %	Adj. SS	Adj. MS	F-value	P-value
Model	9	2595.67	98.95%	2595.67	288.41	52.12	0.000
Linear	3	2403.00	91.60%	2403.00	801.00	144.76	0.000
X1	1	1512.50	57.66%	1512.50	1512.50	273.34	0.000
X2	1	312.50	11.91%	312.50	312.50	56.48	0.001
X3	1	578.00	22.03%	578.00	578.00	104.46	0.000
Square	3	135.67	5.17%	135.67	45.22	8.17	0.023
X1*X1	1	74.40	2.84%	72.03	72.03	13.02	0.015
X2*X2	1	39.70	1.51%	35.10	35.10	6.34	0.053
X3*X3	1	21.56	0.82%	21.56	21.56	3.90	0.105
2-Way Inter.	3	57.00	2.17%	57.00	19.00	3.43	0.109
X1*X2	1	16.00	0.61%	16.00	16.00	2.89	0.150
X1*X3	1	25.00	0.95%	25.00	25.00	4.52	0.087
X2*X3	1	16.00	0.61%	16.00	16.00	2.89	0.150
Error	5	27.67	1.05%	27.67	5.53		
Lack of fit	3	23.00	0.88%	23.00	7.67	3.29	0.242
Pure-Error	2	4.67	0.18%	4.67	2.33		0.000
Total	14	2623.33	100.00%				0.000
Model Summary		S	R ²	R ² (adj.)	Press		R ² (pred.)
		2.35230	98.95%	97.05%	378.5		85.57%

According to **Table 7**, it is noticed that catalyst dosage (Fe₂O₃@CeO₂; 1:2 ratio/AC) (X₁) was shown to be the most significant parameter influencing the RE% with a percentage contribution of 57.66%, demonstrating the catalyst's participation in the breakdown of organic pollutants. With a percentage contribution of 22.03%, the influence of H₂O₂ dose (X₃) was at the second level, but pH (X₂) had a smaller impact on the RE% with a percentage contribution of 11.91%. Furthermore, all 2-way interactions are non-significant since their contribution to the RE% was so negligible—0.109%—that it could be disregarded [26].

Figure 7 (Pareto chart) reveals that the quadratic term of the catalyst dosage (A) exerts the greatest influence on COD removal, followed in descending order by the quadratic term of the pH(C), the linear effect of hydrogen peroxide (H₂O₂) dosage (B), and the significant two-factor interactions catalyst dosage × pH (A × C). By contrast, the weakest effects on the response are associated with catalyst dosage × (H₂O₂) dosage (A × B) and (H₂O₂) dosage × pH (B × C), the linear catalyst percentage (C), the linear reaction time (A), and the interaction time × catalyst percentage (A × C), all of which fall below the statistical significance threshold (α = 0.05).

Figure 8 depicts the optimal values of catalyst dosage (Fe₂O₃@CeO₂; 1:2/AC), H₂O₂ dosage and pH proposed by the BBD method, where y: represents the highest proposed RE% and the optimum value are: catalyst dosage (Fe₂O₃@CeO₂; 1:2 ratio/AC) = 1.5 g/l, H₂O₂ dosage = 0.5897 g/l, and pH = 3 where D-parameter is 1. Where, d represents the working accuracy when it is equal to 1.

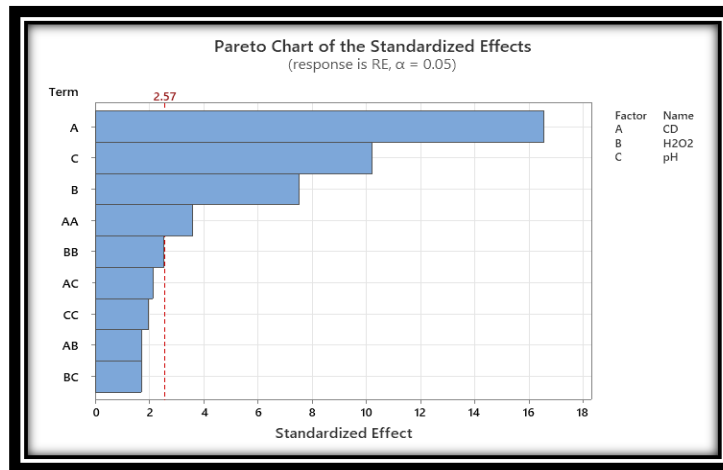


Figure 7. Pareto diagram for the standardized effects

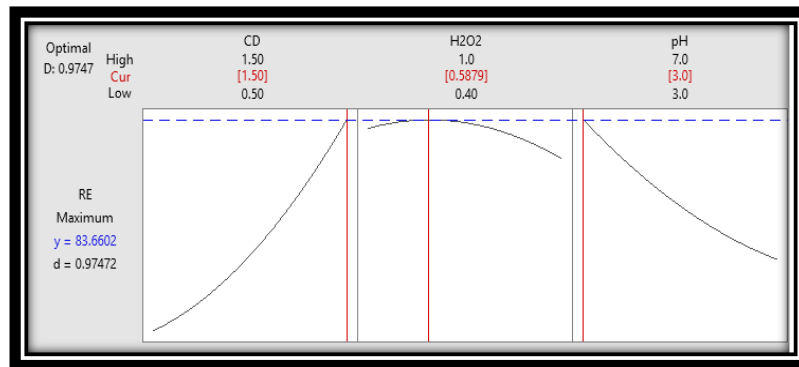


Figure 8. Response optimization plot

Figure 9 compares the COD percent figures for actual and expected elimination efficiency. With $R^2 = 0.9895$, which provides a strong indicator that the expected values are extremely near to the actual ones, the figure demonstrates that the predicted and real values are in good agreement.

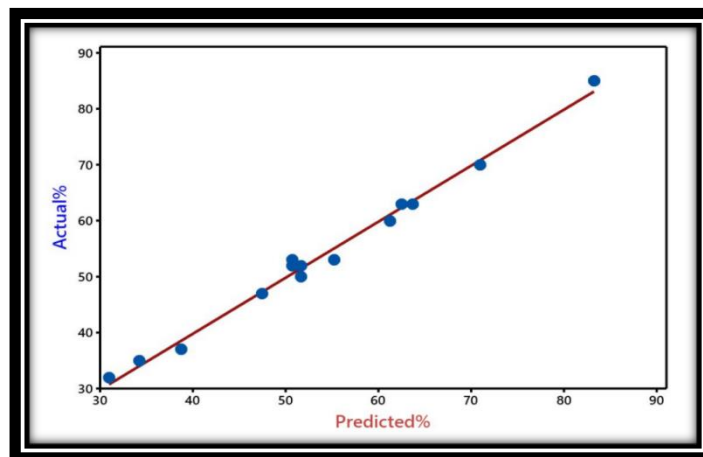


Figure 9. Plot of the experimental versus the predicted values of the removal efficiency

3.3.2. Operating parameters' impact

To determine the impact of process factors and their combinations on the RE%, a graphical representation of the quadratic model based on RSM was used. Figure (10-a,b) illustrates the combined impacts of catalyst dosage ($\text{Fe}_2\text{O}_3@ \text{CeO}_2$; 1:2 ratio/AC) and hydrogen peroxide (H_2O_2) dosage on the RE% at the middle value

of pH (5). The response surface plot is displayed in figure (10-a), and the corresponding contour sketch is shown in figure (10-b). From Figure (10- a), it can be seen that RE% increase with increase catalyst dosage((Fe₂O₃@CeO₂;1:2/AC) because and decrease with increasing hydrogen peroxide (H₂O₂) dosage. Increasing catalyst dosage due to increasing the surface area available for pollutant adsorption and the number of reaction sites and due to increase RE%. When H₂O₂ is increases, it consumes hydroxyl radicals instead of producing them therefore; RE% decreases [27]. Consistent with findings in heterogeneous Fenton systems, COD removal efficiency often reaches a maximum at an optimal H₂O₂ dosage and then decreases at higher dosages, due to •OH scavenging by excess H₂O₂ and unproductive decomposition pathways [27-28]. **Figure (10-b)**, It is clear that within a region in which catalyst dosage ((Fe₂O₃@CeO₂; 1:2/AC) is (1.4-1.5) g/l and (H₂O₂) dosage from (0.4-0.7) g/l., R.E% >70% could potentially be attained. As revealed by previous works, the heterogenous fenton degradation rate rises with an increase in the dosage of the catalyst and H₂O₂ dosages up to the optimal value.

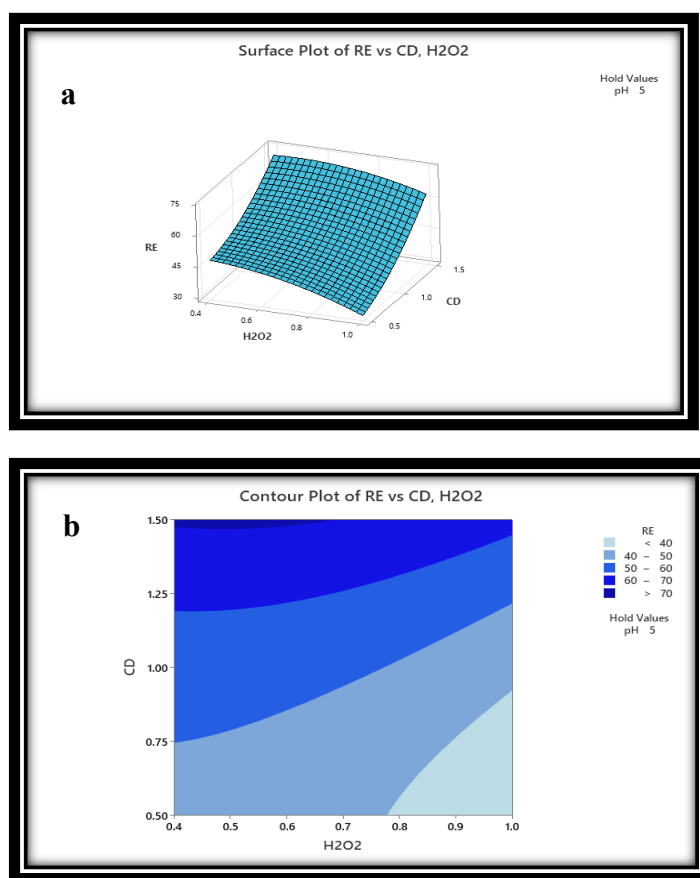


Figure 10. shows the interaction between catalyst dosage and (H₂O₂) dosage in three dimensions (a) and the contour plot between catalyst dosage and (H₂O) dosage (b)

Figure (11-a) demonstrates that an increase in catalyst dosage leads to a rise in RE% ,while esclation in pH is attributed to decrease in RE% at hold value of (H₂O₂) dosage at 0.7 g/l. With respect to and figure(11-b) it is clear that R.E% >80 % might be obtained within a region in which catalyst dosage from (1.4-1.5) g/l and pH value from (3-3.5). Same results were obtained by (Xiaobin Hua et al., 2011)[28], where degradation of methyltestosterone (MT) was studied using ferroferric oxide nanoparticles decorated multiwalled carbon nanotubes (Fe₃O₄/MWCNTs), at catalyst dosage (0.2 g L⁻¹, 1.0 g L⁻¹ and 2.0 g L⁻¹) as a heterogenous fenton process. With an increase in catalyst dosage from 0.2 g L⁻¹ to 2 g L⁻¹, it was found that MT degradation rose from 62.8% to 85.9%. This was caused by an increase in the number of active sites for MT adsorption and, possibly, for the production of •OH.

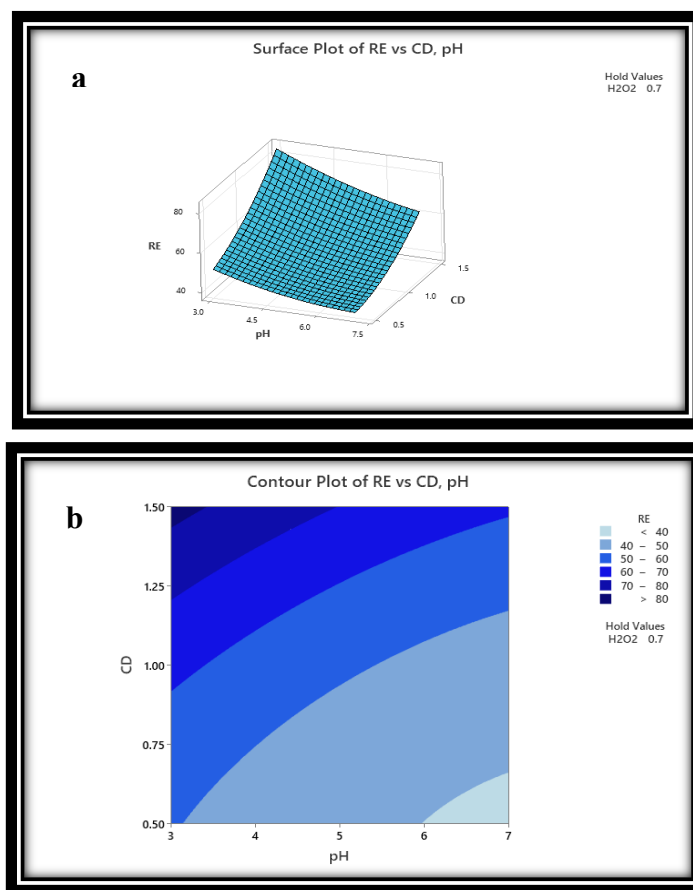


Figure 11. shows the relationship between catalyst dosage and pH in three dimensions (a) and as a contour plot (b)

Regarding **Figure (12 - a)**, it is clear that an escalation in the pH value leads to decreasing in RE%, while regarding (H₂O₂) dosage it can be observed that RE% increases up to 0.5 g/l and then begins to decreasing for end of (H₂O₂) dosage. The contour plot results in **Figure 12-b** indicate that RE% >60 is achievable within a region in which (H₂O₂) dosage is (0.9 - 1) g/l and pH is (5.5 - 7) at hold value for catalyst dosage is 1 g/l. Numerous researchers have documented that pH can also affect heterogeneous Fenton reactions. The impact of pH on the photodegradation of azo dye MY10 in the H₂O₂/α-FeOOH system was documented by (He et al., 2002) [29]. In 120 minutes, the efficiency dropped from roughly 100% to 65% as the pH rose from 5 to 9. A lower pH (<8) results in a positively charged surface because the point of zero charge (PZC) of α-FeOOH is around 8.0. This enhances the anionic dye MY10's adsorption. According to Zhao et al. (2008), the pH change clearly affected both the selectivity of the reaction on the catalyst surface and the mechanism of substrate adsorption on the catalyst from the perspective of pH_{Zpc} of iron oxides [30].

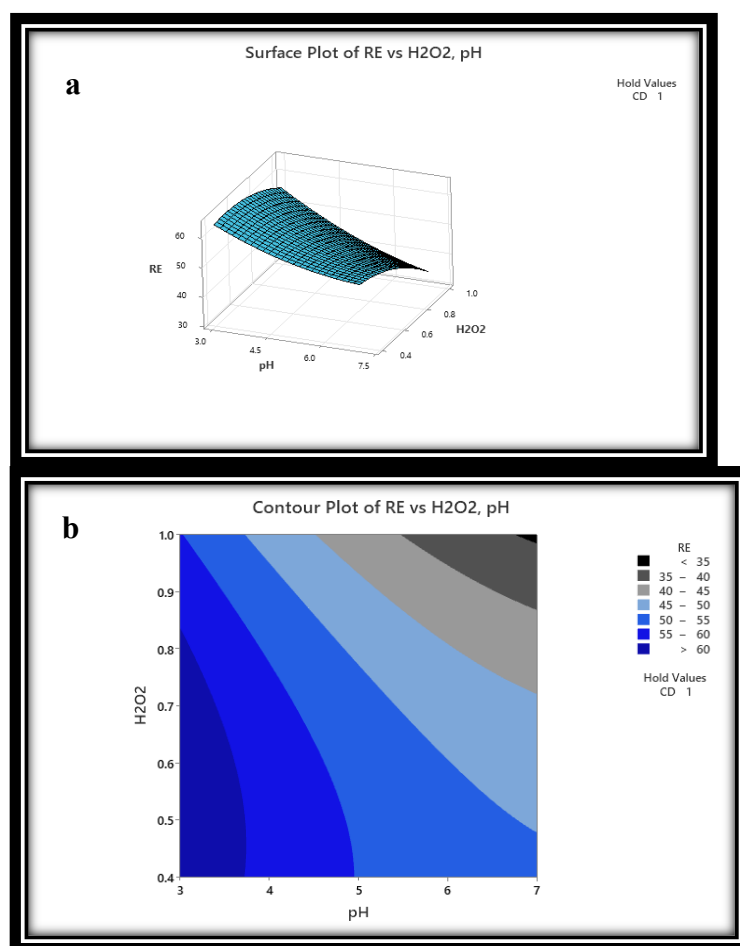


Figure 12. shows the relationship between (H₂O₂) dose and pH in three dimensions (a) and as a contour plot (b)

(Xiaobin Hua et al.) investigated the breakdown of methyltestosterone (MT) utilizing multiwalled carbon nanotubes coated with ferroferric oxide nanoparticles (Fe₃O₄/MWCNTs), at pH values , 2.5, 3.5, 5.0 and 8.0. It was noticed over 90% within 30 min at pH 2.5 and 3.5 [28]. The findings demonstrated that the heterogeneous Fenton process's reaction efficiency tended to peak at about pH 3 and declined with rising pH.

3.3.3. Optimization

The goal of any optimization process is to maximize the response's value. As a result, RE% with a desire function (DF) of 1.0 was proposed as the maximum. Minitab-19 software's response optimizer was used to determine optimization. Table 8 provides an explanation of the optimization outcomes. The optimum theoretical elimination of RE% was found to be 83.66%, which could be achieved at catalyst dosage (Fe₂O₃@CeO₂; 1:2 ratio /AC) = 1.5 g/l, H₂O₂ dosage = 0.5897 g/l, and pH = 3.

Table 8. Optimization of Response depending on RE%

Response	Aimed	Lower	Target	Upper	Weight	Importance	
RE (%)	Max.	32	85	-	1	1	
Results				Parameters			
Fe ₂ O ₃ -CeO ₂ ; 1:2)/AC (g/l)	H ₂ O ₂ (g/l)	pH	RE% Fit	D _F	SE Fit	95% CI	95% PI
1.5	0.5878	3	83.66	1	2.11	(78.23, 89.09)	(75.53, 91.79)

3.3.4. Results validation

Table 9 shows that in order to validate the optimization results, two tests were conducted using the optimized parameters. The average COD removal effectiveness of 85% was reached at 90 minutes of the heterogeneous fenton process, which is consistent with the range of the optimal value derived from optimal results (**Table 8**). Therefore, utilizing Fe₂O₃@CeO₂ in a 1:2 ratio and AC as a catalyst, Box-Behnken design with DF can serve as an efficient approach feature for maximizing RE% by heterogeneous fenton process.

Table 9. Confirmative runs for optimum of RE%

Run	Fe ₂ O ₃ -CeO ₂ ; 1:2/AC (g/l)	H ₂ O ₂ (g/l)	pH	COD _r (ppm)	RE%
1	1.5	0.5878	3	116	85
2	1.5	0.5878	3	110.2	80.7

A comparison of the photocatalysis-treated and untreated effluent is presented in Table 10. Table 10 shows that the treated pollutants have improved characteristics with a final COD value of 116 ppm, a RE% of 85%, and a turbidity removal of more than 96%.

Table 10. Comparison of untreated and treated wastewater using heterogeneous Fenton method.

Test	Untreated	Treated by (Fe ₂ O ₃ @CeO ₂ ; 1:2)/AC	Unit
pH	7.2	8.6	-
Temperature °C	14	28	°C
TDS	1669	701	Ppm
COD	776	116	Ppm
Turbidity	117	4.3	NTU

3.3.5. Fe₂O₃@ CeO₂; 1:2 ratio /AC nanomaterials recycling

The activity of Fe₂O₃@ CeO₂; 1:2 ratio /AC nanomaterials in degradation petroleum refinery wastewater was implemented using a number of working cycles. In each cycle the catalyst was separated from the solution then washed thoroughly with deionized water and calcined at 600 ° C for 4 h^[31]. The calcination process was performed to regenerate the catalyst due to blocking of active sites by organic materials during the treatment. **Figure 13** displays the impact of cycles number on the removal efficiency of COD where loss of performance the catalyst is low through the successive treatment confirming the good activity of the catalyst^[32].

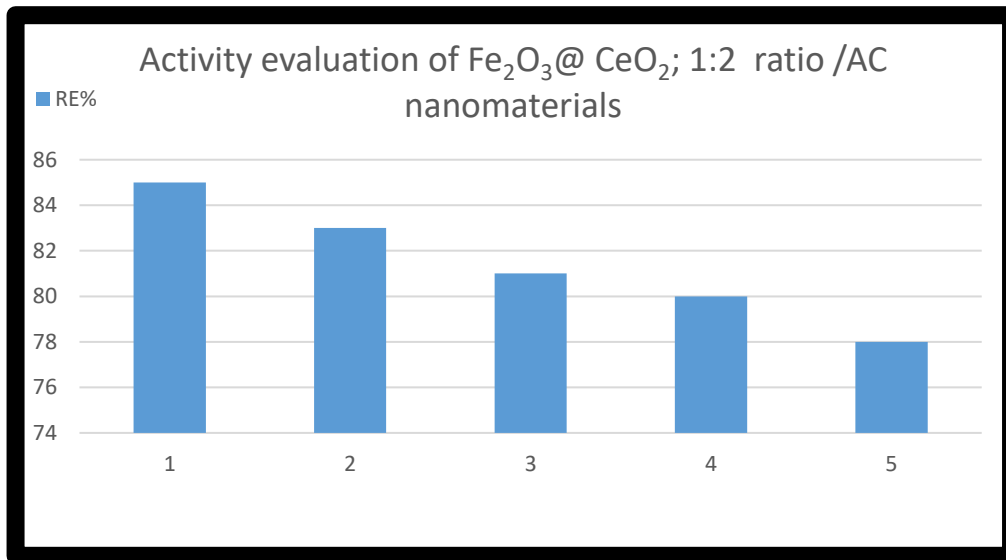


Figure 13. Activity evaluation of Fe₂O₃@ CeO₂; 1:2 ratio /AC nanomaterials

3.3.6. Kinetic Study

To get the proper reactor design, it is essential to ascertain the kinetic coefficients involved in a process. In terms of several intermediates and ultimate products, the reactions in the heterogeneous Fenton process for breaking down petroleum refinery effluents are incredibly complicated [33].

In heterogeneous Fenton processes, the breakdown of organic contaminants is often approximated using a pseudo-first-order kinetic model, particularly when both the oxidant (H₂O₂) and the available catalytic active sites are present in excess compared to the pollutant. Under these circumstances, the concentration of hydroxyl radicals (•OH) remains nearly constant, resulting in an apparent first-order dependence on the pollutant concentration.

Nevertheless, in this study, the obtained correlation coefficients (R²) do not consistently reach sufficiently high values to firmly validate a strict pseudo-first-order kinetic description. Accordingly, the manuscript has been revised to address this point more carefully. First, the justification for applying the pseudo-first-order model has been expanded to clarify its underlying assumptions and inherent limitations in heterogeneous Fenton systems. Second, the description of the model has been refined, emphasizing that it serves as an approximate representation of the kinetics rather than a conclusive mechanistic interpretation. Finally, the discussion now explicitly acknowledges the moderate R₂ values and highlights the associated limitations in fitting the experimental data to this model.[26]

In the advanced oxidation process, it was discovered that the attack of hydroxyl radicals on organic molecules and their byproducts was first-order with respect to the decay of COD, where the concentration of hydroxyl radicals is constant while processing Equ.(4) and Equation (5)

$$r = \frac{dCOD}{dt} = k[HO^{\bullet}]^{\alpha} COD = k_{app} COD \quad (4)$$

$$COD = COD_o \exp(-k_{app}t) \quad (5)$$

The plot of ln (COD_o/COD) over time can be used to compute k_{app}, a pseudo-first-order kinetic constant in this equation, which is referred to as a pseudo-first-order kinetic.

Numerous heterogeneous Fenton reactions of aquatic organics have been satisfactorily described by pseudo-first-order kinetics [28]. The kinetics were examined at three catalyst dosage values (0.5, 1, and 1.5) g/l at 0.5879 g/L H₂O₂ dosage and pH of 3 because catalyst dosage is the primary determinant in this process, according to ANOVA data (Table 7). The COD decay over time for heterogeneous Fenton at various catalyst

dosages is shown in **Figure 13**. It is evident that for various catalyst dosage values, the degradation tends to be roughly exponential.

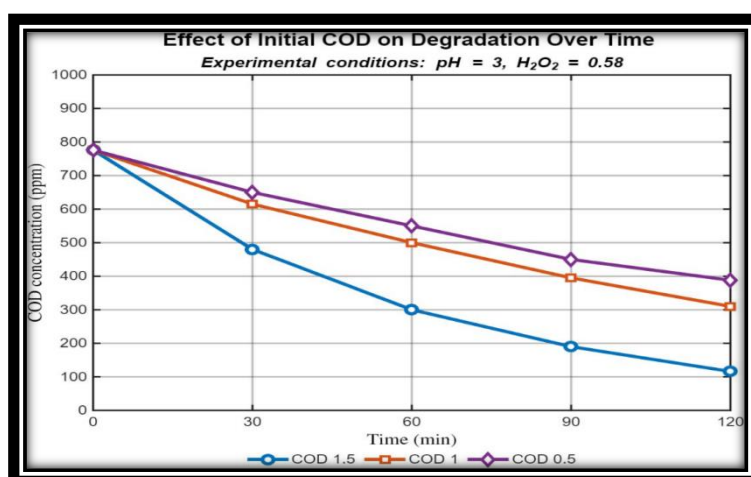


Figure 13. COD degradation over time with heterogeneous Fenton at varying catalyst dosages

The relationship between $\ln(\text{COD}/\text{COD}_0)$ and time at various catalyst dosage values is depicted in **Figure 14**. With an R^2 of 0.984-0.989, it was evident that the results were close-fitting. The application of pseudo first-order kinetics to explain the COD degradation in the $\text{Fe}_2\text{O}_3@\text{CeO}_2$; 1:2 ratio/AC system is confirmed by the high values of R^2 . These findings also demonstrated that heterogeneous Fenton is a potential method for eliminating different chemical components from PRWW.

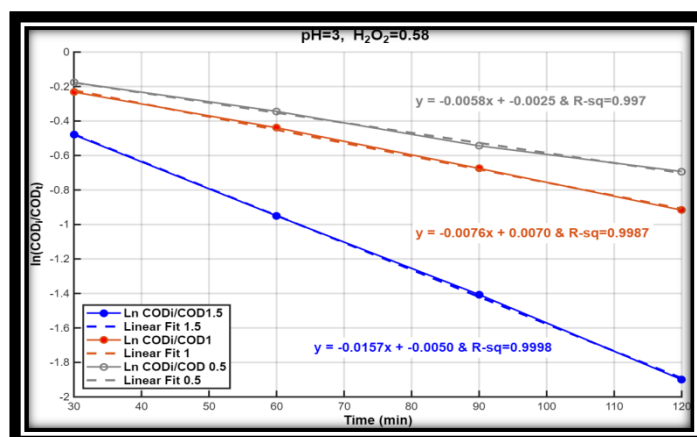


Figure 14. Heterogeneous Fenton pseudo-first order model for COD degradation at varying catalyst dosages

4. Mechanism of CeO_2 promoting Fe_2O_3 Fenton activity

CeO_2 has a key function in the system owing to its reversible $\text{Ce}^{3+}/\text{Ce}^{4+}$ redox pair and its ability to store and release oxygen, both of which assist in converting Fe^{3+} back to Fe^{2+} and thus intensify the Fenton cycle. In particular, Ce^{3+} acts as a reducing agent for Fe^{3+} , enabling the sustained formation of hydroxyl radicals ($\bullet\text{OH}$) through the conventional Fenton pathway. Moreover, the presence of oxygen vacancies in CeO_2 enhances interfacial electron transfer and improves the activation efficiency of H_2O_2 . The overall synergistic mechanism may be represented by the following reactions:

- $\text{Fe}^{2+} + \text{H}_2\text{O}_2 \rightarrow \text{Fe}^{3+} + \bullet\text{OH} + \text{OH}^-$
- $\text{Ce}^{3+} + \text{Fe}^{3+} \rightarrow \text{Ce}^{4+} + \text{Fe}^{2+}$
- $\text{Ce}^{4+} + \text{e}^- \rightarrow \text{Ce}^{3+}$ (regenerated through surface processes)

With respect to hydroxyl radical identification, we acknowledge that direct detection would provide stronger support for the proposed mechanism. However, due to experimental constraints, radical scavenging or trapping tests were not performed in the initial version of the work.^[34-35]

5. Conclusion

The feasibility of heterogeneous Fenton process using Fe₂O₃ @ CeO₂; 1:2 ratio /AC as nanocatalyst was examined successfully in treating the effluents of AL-Diwaniyah petroleum refinery. The impacts of four variables (catalyst dosage, H₂O₂ dosage, and pH) on the RE% were studied and optimized via RSM-BBD. Results of ANOVA confirmed that catalyst dosage and pH are the most essential factors that controlled on the mechanism of the heterogeneous Fenton process. While the other factor (H₂O₂ dosage) have the second degree in their impacting on COD removal. The preferred conditions were fixed as: catalyst dosage = 1.5 g/l, H₂O₂ dosage = 0.5878 g/l pH=3 that resulted in optimum RE% of 85%. The model has R² value of 96.33% confirming the successful adopting of RSM in presenting the relation between the variables of process and the response. Using heterogeneous Fenton process results in improving the removal processes in term of the efficiency and cost in comparison with classical Fenton processes. Consequently, adopting the heterogeneous Fenton process could be adopted as a sustainable, alternative, and cost-effective process for treating different sources of wastewaters.

Acknowledgments

The authors are indebted for the help and the technical support provided by Chemical Engineering Department staff at the University of AL-Qadisiyah, Iraq.

Conflict of interest

The authors declare no conflict of interest.

References

1. Zhang, Y., Gao, M. M., Wang, X. H., Wang, S. G., & Liu, R. T. (2015). Enhancement of oxygen diffusion process on a rotating disk electrode for the electro-Fenton degradation of tetracycline. *Electrochimica Acta*, 182, 73-80.
2. Al-Malack, M. H., & Siddiqui, M. (2013). Treatment of synthetic petroleum refinery wastewater in a continuous electro-oxidation process. *Desalination and Water Treatment*, 51(34 - 36), 6580 - 6591.
3. Kavitha, V., & Palanivelu, K. (2004). The role of ferrous ion in Fenton and photo-Fenton processes for the degradation of phenol. *Chemosphere*, 55(9), 1235 - 1243.
4. Al Hashemi, W., Maraqa, M. A., Rao, M. V., & Hossain, M. M. (2015). Characterization and removal of phenolic compounds from condensate-oil refinery wastewater. *Desalination and Water Treatment*, 54(3), 660-671.
5. Aljouboury, D. A. D. A., Palaniandy, P., Abdul Aziz, H. B., & Feroz, S. A. D. A. (2017). Treatment of petroleum wastewater by conventional and new technologies-A review. *Glob. Nest J*, 19(3), 439-452.
6. Dutta, S., Gupta, B., Srivastava, S. K., & Gupta, A. K. (2021). Recent advances on the removal of dyes from wastewater using various adsorbents: A critical review. *Materials Advances*, 2(14), 4497-4531.
7. Malik M. Mohammed, Ali Akber Amooey & Haider Alwan "Electro Oxidation Process for Wastewater Treatment in Petroleum Refineries", 2024, *Pollution* 10 (2), 819-832 [7]
8. Kalash, K. R., Al-Furaiji, M. H., Mter, K. A., Alalwan, H. A., Alazraqi, A. R., Sultan, H. I., & Algam, M. H. (2025). Assessment of hybrid treatment process for high-COD oily wastewater following Iraqi discharge regulations: A case study from Baghdad power plant. *Indian Chemical Engineer*, 1 - 16. <https://doi.org/10.1080/00194506.2025.2579533>
9. Hassan, A. A., Naeem, H. T., & Hadi, R. T. (2018). Degradation of oily waste water in aqueous phase using solar (ZnO, TiO₂ and Al₂O₃) catalysts. *Pakistan Journal of Biotechnology*, 15(4), 927-934.
10. Xu, M., Wu, C. and Zhou, Y., 2020. Advancements in the Fenton process for wastewater treatment. In *Advanced oxidation processes-applications, trends, and prospects*. IntechOpen.
11. Lama, G., Mejjide, J., Sanroman, A. and Pazos, M., 2022. Heterogeneous advanced oxidation processes: current approaches for wastewater treatment. *Catalysts*, 12(3), p.344.

12. Marwa Abd Aljaleel; Hameed Hussein Alwan; "Modeling the Effect of Operation Variables on Copper Ions Removal by Electrocoagulation" 2022 2nd International Conference on Advances in Engineering Science and Technology (AEST)
13. Sata Kathum Ajjam et al.; "Nitrate removal from simulated wastewater by electrocoagulation: Impact of operating parameters on removal efficiency and energy consumption"; South African Journal of Chemical Engineering; Volume 55, January 2026, Pages 1-10
14. Ahmadreza Yazdanbakhsh, et al., 2018 "Performance of granular activated carbon/nanoscale zero-valent iron for removal of humic substances from aqueous solution based on Experimental Design and Response Surface Modeling" Global NEST Journal, Vol 20, No X, pp XX-XX
15. Al-Furaiji, M. H., Alalwan, H. A., Sultan, H. I., & Al-Shaeli, M. N. (2021). Synthesis of ZnO - CoO/Al₂O₃ nanoparticles and its application as a catalyst in ethanol conversion to acetone. Results in Chemistry, 3, 100249. <https://doi.org/10.1016/j.rechem.2021.100249>.
16. Al-Tameemi, H.M., Sukkar, K.A. & Abbar, A.H. Electrochemical Treatment of Petroleum Refinery Wastewater Using SnO₂ and Graphite Anodes. Pet. Chem. 64, 144 - 150 (2024). <https://doi.org/10.1134/S0965544124020075>
17. El-Ghenymy, A., Garcia-Segura, S., Rodríguez, R. M., Brillas, E., El Begrani, M. S., & Abdelouahid, B. A. (2012). Optimization of the electro-Fenton and solar photoelectro-Fenton treatments of sulfanilic acid solutions using a pre-pilot flow plant by response surface methodology. Journal of hazardous materials, 221, 288-297.
18. Evans, M., 2003. Optimization of Manufacturing Processes: A Response Surface Approach. Carlton House Terrace, London.
19. Alalwan, H. A., Sultan, H. I., Al-Furaiji, M. H., & Al-Shaeli, M. N. (2022). Using Box - Behnken experimental design for optimization of gas oil desulfurization by electrochemical oxidation technique. Fuel Processing Technology.
20. Alalwan, H. A., Sultan, H. I., Al-Furaiji, M. H., & Al-Shaeli, M. N. (2023). Methane activation on metal oxide nanoparticles: Spectroscopic identification of reaction mechanism. Particulate Science and Technology, 41(5), 653 - 660. <https://doi.org/10.1080/02726351.2022.2034567>
21. Alalwan, H. A., Sultan, H. I., Al-Furaiji, M. H., & Al-Shaeli, M. N. (2023). Spectroscopic investigation of carbon dioxide interactions with transition metal-oxide nanoparticles. Chemical Engineering & Technology, 46(3), 587 - 594. <https://doi.org/10.1002/ceat.202200355>
22. Alalwan, H. A., Sultan, H. I., Al-Furaiji, M. H., & Al-Shaeli, M. N. (2022). Employing synthesized MgO - SiO₂ nanoparticles as catalysts in ethanol conversion to 1,3-butadiene. International Journal of Nanoscience and Nanotechnology, 18(3), 157 - 166.
23. Huizhi Bao, "Structure-activity Relation of Fe₂O₃ - CeO₂ Composite Catalysts in CO Oxidation" catalysis letters, Volume 125, pages 160 - 167, (2008)
24. Naife, T.M., 2012. ADSORPTION STUDY OF HYDRODESULPHURIZATION CATALYST. Journal of Engineering, 18(01), pp.38-50.
25. Mariana Riboli Nava et al.; "Characterization of CeO₂ - Fe₂O₃ Mixed Oxides: Influence of the Dopant on the Structure" Journal of Photochemistry & Photobiology, A: Chemistry (2022).
26. Asyah R. Flayyih, Ali H. Abbar, "Treatment of petroleum refinery wastewater by a heterogeneous electro-Fenton process using activated carbon loaded with Fe₂O₃-CeO₂ as a catalyst", Results in Engineering, Volume 28, 2025,
27. Zheng-nan Sun, Qi Yang, Dong-li Ji, Lin Zheng., "Degradation of 3,4- Dichlorobenzotrifluoride by Fe₃O₄/CeO₂-H₂O₂ Heterogeneous Fenton-Like Systems"; PubMed, 2015 Jun;36(6):2154-60.
28. Xiaobin Hua et al., 2011 "Adsorption and heterogeneous Fenton degradation of 17 α -methyltestosterone on nano Fe₃O₄/MWCNTs in aqueous solution" Applied Catalysis B: Environmental 107 (2011) 274 - 283.
29. J. He, W.H. Ma, J.J. He, J.C. Zhao, J.C. Yu, Appl. Catal. B: Environ. 39 (2002) 211 - 220.
30. Y.P. Zhao, H.Y. Hu, Appl. Catal. B: Environ. 78 (2008) 250 - 258.
31. Ghasemi, Z., Younesi, H., & Zinatizadeh, A. A. (2016). Kinetics and thermodynamics of photocatalytic degradation of organic pollutants in petroleum refinery wastewater over nano-TiO₂ supported on Fe-ZSM-5. Journal of the Taiwan Institute of Chemical Engineers, 65, 357-366
32. De Oliveira, C. P. M., Viana, M. M., & Amaral, M. C. S. (2020). Coupling photocatalytic degradation using a green TiO₂ catalyst to membrane bioreactor for petroleum refinery wastewater reclamation. Journal of Water Process Engineering, 34, 101093.
33. Aljoubury, D.D.A., Palaniandy, P., Abdul Aziz, H.B., Feroz, S., 2015. Evaluating the TiO₂ as a solar photocatalyst process by response surface methodology to treat the petroleum waste water, Karbala Inter. J. Mod. Sci. 1, 78 - 85.

34. Nishanth Thomas, Dionysios D. Dionysiou, Suresh C. Pillai, "Heterogeneous Fenton catalysts: A review of recent advances", Journal of Hazardous Materials, Volume 404, Part B, 2021.
35. Israa Mohammed, Hameed Hussein Alwan and A. N. Ghanim "Using Box-Behnken experimental design for optimization of gasoil desulfurization by electrochemical oxidation technique ," IOP Conf. Series: Materials Science and Engineering 928 (2020) 022158.